Astron. Astrophys. 328, 187–202 (1997)

ASTRONOMY
AND
ASTROPHYSICS

A study of the Chamaeleon star-forming region from the ROSAT all-sky survey⋆

III. High resolution spectroscopic study

E. Covino[1], **J.M. Alcalá**[2,6], **S. Allain**[3], **J. Bouvier**[3,4], **L. Terranegra**[1], **and J. Krautter**[5]

[1] Osservatorio Astronomico di Capodimonte, Via Moiariello 16, I-80131 Napoli, Italy
[2] Max-Planck-Institute für Extraterrestrische Physik Giessenbachstr. 1, D-85740 Garching, Germany
[3] Laboratoire d'Astrophysique, Observatoire de Grenoble, Université Joseph Fourier, B.P. 53X, F-38041 Grenoble Cedex, France
[4] CFH Telescope Corporation, Kamuela, HI USA
[5] Landessternwarte Heidelberg, Königstuhl, D-69117 Heidelberg, Germany
[6] Instituto Nacional de Astrofísica, Optica y Electrónica, A.P. 51 y 216 C.P. 72000, Puebla, México

Received 26 March 1997 / Accepted 30 June 1997

Abstract. We present the results of a high-resolution spectroscopic study on some 70 stars, discovered recently on the basis of the ROSAT all-sky survey spread over a wide area in the Chamaeleon star forming region and classified as new weak-line T Tauri stars.

We refine the previous spectral type classification, based on low-resolution spectra, and characterize each star in the sample according to the Hα line profile.

We use the strength of Li I 6708, compared to Pleiades stars of the same spectral type, as a youth discriminator in order to recognize *bona-fide* pre-main sequence stars. According to the adopted "lithium criterion", more than 50% of the stars in our sample are confirmed to be truly young, PMS stars (most having age less than 5×10^6 yr), while the remaining part seems mostly composed by active, young, foreground main-sequence stars (possibly Pleiades-like), which contaminate the original sample. We confirm the existence of some very young stars far from the main Chamaeleon clouds, while we do not find clear evidence for the presence of post-T Tauri stars in our sample.

We find that 5 stars in the sample are spectroscopic binaries and 1 is a spectroscopic triple system.

We derive radial and rotational velocities for all the stars in sample and analyse their distributions for different spectral type intervals. The radial velocity distribution shows a clear peak at about 15 km s^{-1}, which coincides with the radial velocity of stars and gas in the Cha I cloud. However, the velocity dispersion of the weak-line T Tauri stars appears much broader and, possibly, a second peak is present around 16-18 km s^{-1}.

A clear segregation in radial velocity is observed between the strong-lithium and the weak-lithium stars, with the former showing radial velocities which, in most cases, fall in the interval 12<RV [km/s] < 18, consistent with the radial velocity peak observed for the Cha I dark cloud, and the latter having somewhat different and more widely spread radial velocities. Some strong-lithium stars having radial velocities outside the aforementioned interval might be unrecognized spectroscopic binaries, but they may also be considered good candidates to be run-away T Tauri stars.

The $v \sin i$ distribution of the confirmed WTTS is found to resemble very closely that of other pre-ROSAT PMS stars.

We conclude that the whole star forming region has a common origin, possibly related to the impact of a high-velocity cloud with the galactic plane.

Key words: stars: formation; pre-main sequence; late type; rotation – ISM: Chamaeleon clouds

1. Introduction

X-ray observations from the EINSTEIN satellite first (Walter et al., 1988; Feigelson 1987, and references therein), and, quite recently, new X-ray data from the ROSAT all-sky survey (Krautter et al., 1994; Krautter 1996, and references therein) called the attention to a previously unnoticed population of pre-main sequence (PMS) stars, the weak-line T Tauri stars (WTTS).

This new class of low-mass PMS stars lack both strong emission lines and IR excesses typical of classical T Tauri stars (CTTS), and most of them have been discovered only thanks to their solar-like coronal X-ray emission.

A long term project aiming to identify new WTTS on the basis of X-ray data from the ROSAT all-sky survey (RASS)

Send offprint requests to: E. Covino

⋆ Based on observations collected at the European Southern Observatory at La Silla, Chile

started in 1990 (Krautter at al. 1994). Some hundreds of strong-lithium stars, classified as new WTTS, have been discovered by means of low-resolution spectroscopy in the Chamaeleon (Alcalá et al. 1995; henceforth Paper I), Lupus (Krautter et al., 1997), Taurus-Auriga (Wichmann et al., 1996), Orion (Alcalá et al., 1996) star forming regions (SFR's)

The discovery of large numbers of WTTS in all the nearby SFR's investigated, also very far from dense star forming cloud cores, opens a large debate about the origin of these objects, and different models trying to explain the presence of very young stars far from molecular clouds have already been proposed (Sterzik & Durisen 1995, Feigelson 1996). On the other hand, in some extreme cases, the PMS nature of these stars has even been put into question (Briceño et al. 1997, hereafter, Br97). There are two main causes which nourish all this debate and they are the following: first, the uncertainty on the distances (as initially pointed out by Alcalá et al. 1997, henceforth Paper II) and, second, the relatively low spectral resolution used for prime identification of the newly discovered WTTS candidates (as advanced by Br97).

The strongest argument in favor of the PMS nature of the widely spread WTTS is that they show a late type spectrum and an intense lithium absorption line (Paper I; Wichmann et al. 1996; Krautter et al. 1997). Assuming that these stars are physically associated to the respective SFR, it is indeed found that they lie well above the ZAMS with typical T Tauri ages (Paper II; Wichmann et al. 1997; Kunkel 1996). Soderblom et al. (1993) have shown that stars in clusters like α Per and the Pleiades (about one order of magnitude older than typical WTTS), show lithium absorption with a large scatter which can be attributed to the spread in masses and rotation rates. This would rise the question whether some of the stars classified as WTTS are in reality older, active ZAMS (or Pleiades-like) stars located at smaller distances from the Sun than previously assumed.

It seems then rather obvious that the easiest way to clarify the nature of the presumed WTTS stars is to study them with high enough spectral resolution in order to discriminate unambiguosly between truly young, PMS stars, and other chromospherically active stars, which might be contaminating the sample, as well as to investigate their kinematics (through radial velocitiy and proper motion studies), and try to establish eventual relationship to any nearby star formation region.

But there is also another very important reason for studying these stars by means of high-resolution spectroscopy, and it is the following. If these stars are really young, then they provide a rather conspicuous sample in which the rotation properties of low-mass PMS stars can be investigated extensively and the problem of the PMS rotational evolution can then be addressed for the first time on a large observational basis.

An aspect of particular interest is that rotational data for the new WTTS are expected to fill in, at least to some extent, the gap in the rotational evolution of young stars in the age range between the T Tauri phase (a few 10^6 to 10^7 yr) and the youngest MS clusters (5×10^7 yr). This is very important because the observational gap coincides with the age interval in which large changes in the surface rotational velocity of a star occur as a consequence of internal structural modifications (which lead to variations in the moment of inertia of the star), as well as of angular momentum transfer and/or angular momentum loss mechanisms, as widely discussed recently by Bouvier (1994) and Keppens et al. (1995). To this respect, it is necessary to gather rotational data for large samples of WTTS, as well as to provide reliable estimates of masses and ages for these stars, in order to test the current rotational evolution models and set constraints on the mechanisms which control the angular momentum evolution of low mass stars during the PMS phase.

A rather intriguing question, in fact, is represented by the different rotation properties observed in classical and weak-line T Tauri stars (TTS). Recent studies of rotational modulation of TTS in the Taurus-Auriga star forming region (Bouvier et al. 1993; 1995), suggest that the distributions of the rotation periods of CTTS and WTTS are different with WTTS being, on average, faster rotators than CTTS. This result has been confirmed also in other SFR's (Choi & Herbst 1996). This difference could be considered as an indication that WTTS spin-up freely as they contract toward the ZAMS, while CTTS are prevented from doing so because of the presence of the disk (ref. Bouvier & Forestini 1994).

Thus, high-resolution spectroscopy appears the most appropriate means to clarify the real nature of these stars, allowing to study at the same time the kinematics (through radial velocity determinations), the rotation (by obtaining projected rotational velocities, $v \sin i$), the abundance of lithium, and, last but not least, to single out multiple spectroscopic systems.

In the present paper we derive radial and rotational velocities for a large sample of WTTS candidates in the Chamaeleon SFR and analyse their distributions in connection to other stellar properties. Derivation of lithium abundances and the connection between lithium depletion, rotation and activity will instead be the subject of a forthcoming paper (Magazzù et al. in preparation).

The plan for this paper is the following. In Sect. 2 we present our sample and in Sect. 3 describe the observations. In Sect. 4 we discuss the Hα emission profiles and lithium equivalent widths. We describe the derivation of radial and rotational velocities in Sects. 5 and 6, respectively, and present the results in Sect. 7. Discussion and conclusions are presented in section 8 and our main results are then summarized in Sect. 9.

2. The sample

Using the RASS data and ground-based follow-up observations, Alcalá et al. (1995) report the discovery of 77 lithium-rich stars widely spread over about 170 square degrees in the Chamaeleon cloud complex. They report spectroscopic and photometric data for these stars and classify them as WTTS.

Seventy-one stars reported in Paper I constitute the primary data base for the present investigation. Additionally, we have included in our sample three stars in the Cha I cloud: the star CHX18N, a WTTS discovered on the basis of *Einstein* data (Walter 1992) and detected by the RASS, the star F34, originally

Table 1. Journal of observations

Date	instrum. config.	Sp. Range (Å)	echelle orders ##	CCD
1994 Jan 31 - Feb 1	CASPEC + short camera	5400-8000	103-69	TK512
1995 Apr 13 - 15	CASPEC + short camera	5800-8500	98-67	TK512
1996 Jan 29 - 31	CASPEC + long camera	5400-8000	105-73	TK1024AB

classified as a field star by Whittet et al (1987), and the star B33, detected in a ROSAT pointed observation (Zinnecker et al. in prep.), which showed a strong X-ray flare. The star F34 was later indicated as a possible Cha I member by Whittet et al. (1991). However, this star was not detected in the RASS, but it was in two ROSAT pointed observations by Feigelson et al. (1993). Its PMS nature was then confirmed by Alcalá (1994) on the basis of mid-resolution spectroscopic observations. For that reason we decided to include it in our observational sample.

The spectral classification of the stars in the sample is given in Paper I. The mid-resolution spectra reported there were used to carry out a careful revision of the previous classification, using the library of stellar spectra by Jacoby et al. (1984), available in digital form. A first-guess spectral type was assigned by visual inspection. Then, an iterative comparison was carried out using the following procedure: each one of the mid-resolution spectra was normalized to the continuum; the guess spectral type standard spectrum was normalized in the same way and rebinned to the same resolution as the mid-resolution spectrum. An overplot of the two normalized spectra allows a direct match of the spectral features and to reject or accept the guess spectral type. The spectral type of the standard which matches more closely the features of the problem star was then assigned to the latter. Finally, a division of the chosen (normalized and rebinned) standard spectrum by the mid-resolution normalized spectrum, yields indication on the goodness of the spectral classification. The spectral type was accepted if the residuals in the division were less than about 10%. This classification leads to the spectral types reported in Table 2. In most cases the previous classification is confirmed and only in a few cases, where the signal to noise ratio of the mid-resolution spectrum is less than about 20, a difference of a few subclasses is found.

The procedures described in Paper II were followed to derive stellar effective temperatures and luminosities, using these new spectral types and the photometric data reported in Paper I. Since the spectral type classification does not differ significantly from the previous one, the effective temperatures, luminosities and extinction values are practically the same, within the errors, as those reported in Paper II.

3. Observations and data reduction

This investigation is based on high-resolution spectroscopic observations carried out at the European Southern Observatory, La Silla (Chile) with the ESO 3.6m telescope during three nights in 1995 (April 13 to 15) and three nights in 1996 (January 29 to 31). Additional data from a previous run conducted with the same instrumentation on two nights in 1994 (January 31 and February 1) are also used in this work. In the 1994 and 1995 runs, the Cassegrain Echelle Spectrograph (CASPEC) in the short camera configuration and with the red cross-disperser was used, equipped with a 31.6 gr/mm echelle grating. At that time, the detector was a Tektronix TK512 CCD of 512 $\times$ 512 pixels of $27\mu m \times 27\mu m$ (ESO # 32) (Pasquini & D'Odorico, 1989). In 1996, CASPEC was used in the long camera configuration in combination with a CCD Tektronix TK1024AB of 1024×1024 pixels (pixel size 24 $\mu m \times 24\mu m$, ESO # 37) as a detector. A slit width of $300\mu m \times 700\mu m$ (corresponding to 2.1 arcsec $\times$ 5 arcsec on the sky) was used at all times for the observations, yielding a nominal resolving power, $\lambda/\Delta\lambda$, of about 20,000. The wavelength range covered was 5800-8500 Å (echelle orders 98 to 67) in the 1995 run and 5400-8000 Å (echelle orders 103 to 69) in the 1994 and 1996 runs.

The journal of the observations and the instrumental set-up are summarized in Table 1.

Typical integration times were 30-45 min, and a S/N ratio larger than 100 was normally achieved for 12-13 mag stars.

Thorium-Argon calibration lamp and quartz lamp flat-field exposures were also always taken immediately before each stellar exposure at the same telescope position. For longer exposures (e.g., $>$ 45 min), calibrations were also taken immediately after the science exposure. However, no systematic difference was really noticed between the two calibration exposures.

A set of radial velocity and $v \sin i$ standard stars of different spectral types were also observed during each run with the same instrumental set-up.

The data reduction was performed at ESO-Garching using the echelle reduction package available within the Munich Image Data Analysis System (MIDAS, version November 1995), plus some specially deviced procedures making use of the algorithms prescribed by Verschueren & Hensberge (1990) for background subtraction and optimal order extraction. The detailed reduction of the CASPEC spectra included the following steps: 1) localization of the echelle orders, 2) fitting and subtraction of the background from all frames, 3) fitting of the blaze function, 4) extraction of echelle orders, 5) wavelength calibration, using the Thorium-Argon calibration exposures, and finally, 6) merging of the orders. The resulting wavelength-calibrated, merged spectra are also already normalized to the continuum.

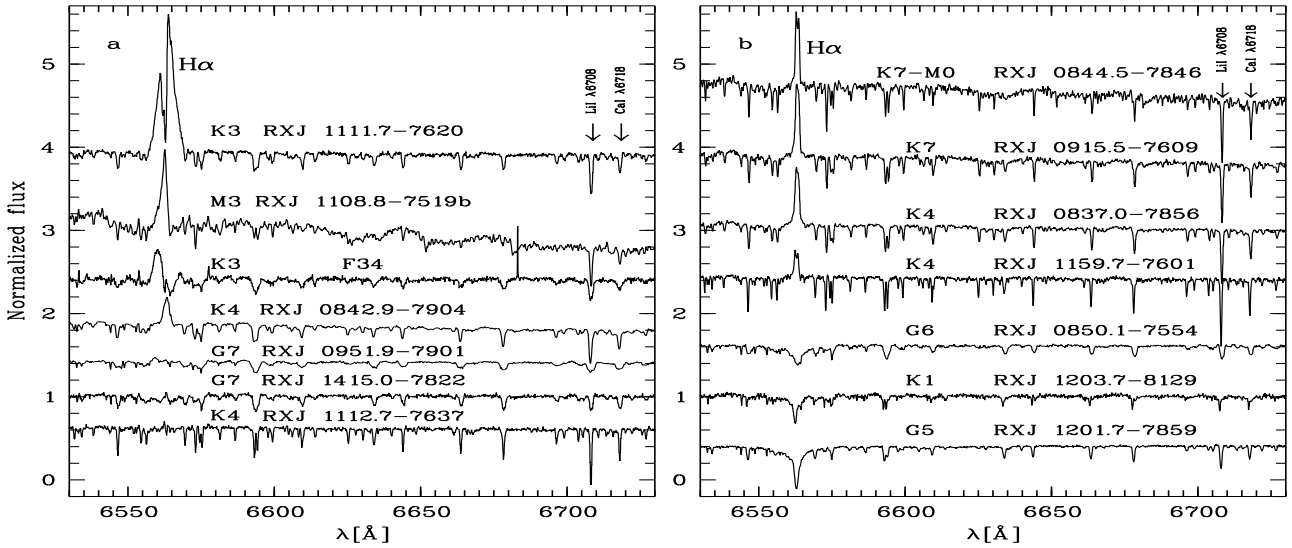

Fig. 1. Sample of high resolution spectra in the range from Hα to Ca I 6718 Å.

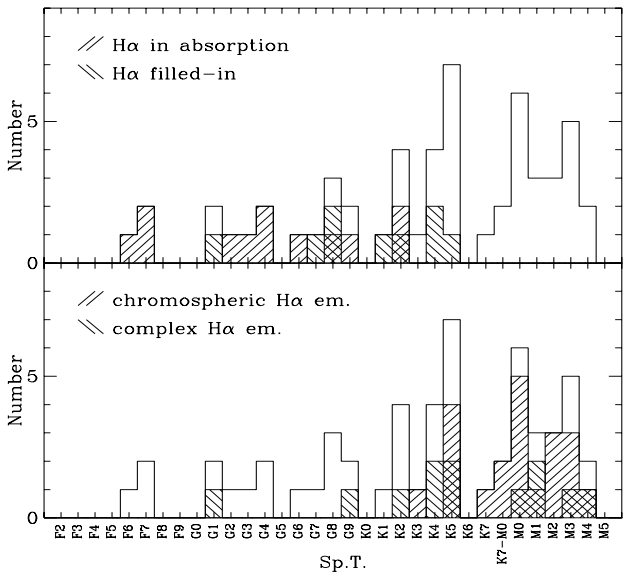

Fig. 2. Spectral type distribution for different types of Hα line profiles. Upper panel: the thin solid line represents the entire sample; the 135° hatched area indicates stars with Hα in absorption; the 45° dashed line area indicates stars with Hα line filled in with emission; lower panel: the thin solid line represents the entire sample; the 135° dashed line area indicates stars with chromospheric-like Hα emission; the 45° hashed area represents stars with broad and/or asymmetric Hα emission.

4. Hα line profiles and Lithium equivalent widths

4.1. Hα line profiles

We examined the Hα profiles for the sample in Chamaeleon, and what appears particularly striking is that, although in most cases the equivalent width of the emission line is less than 5 Å, different kinds of Hα line profile can be distinguished, which can be schematically reconducted to one of the following four groups:

1) stars having Hα line in absorption;
2) stars having Hα filled in with emission;
3) stars showing a quite narrow and symmetric (typically chromospheric) Hα emission;
4) stars with rather complex Hα line profile (e.g., presenting different kinds of asymmetries, double peaks, multiple absorption components, etc.) suggesting that other phenomena, possibly related to a residual circumstellar accretion disk, may still be important.

Only four stars in our sample show a clear indication of an infrared excess, and all of these have Hα in emission (namely, RXJ 1001.1-7913, CHX18N, F 34, and T Cha). The spectral energy distributions of these stars are shown in Fig. 5 of Paper I.

Examples of the most typical profiles in each of the above mentioned categories are shown in Fig. 1.

For stars showing the first three types of profile, the PMS nature relies mainly on the presence of strong lithium absorption line λ 6708 (this is examined in detail in Sect. 7.2). For the fourth group, the complex line profile is reminiscent, in most cases, of those displayed by CTTS and this might represent a further indication of the PMS nature of a star.

The spectral type distributions for the different kinds of Hα line profile is shown in Fig. 2. In the upper panel, the 135° hatched area indicates stars with Hα in absorption (group 1), and the 45° dashed line area stars with Hα line filled-in with emission (group 2); in the lower panel, the 135° dashed line area indicates stars with chromospheric-like Hα emission (group 3), and the 45° hashed area represents stars with broad and/or asymmetric Hα emission. In both panels the thin solid line represents the whole sample.

What is apparent from these spectral type distributions is that stars with Hα filled-in or in absorption (e.g. groups 1 and 2) dominate among earlier types, while stars belonging to the

third group (e.g., chromospheric Hα) clearly dominate among later spectral types. Finally, complex Hα emission seem to be more common among stars of late to intermediate spectral type. This behaviour is consistent with, and mainly reflects, the dependence of stellar continuum and of photospheric Hα absorption on spectral type as well as on the rotational status of a star.

The chromospheric activity-rotation connection in this sample of stars will be studied somewhere else by using Hα emission and X-ray fluxes as activity diagnostics.

4.2. Lithium equivalent widths

The presence of strong absorption in the Li I resonance line at λ 6707.8 Å represents the most important discrimination criterion for identifying young, low-mass PMS stars (D'Antona & Mazzitelli 1984, Strom et al. 1989).

It is well known in fact that, for Population I stars, the abundance of lithium depends on mass and age, since lithium is easily destroyed by convective mixing in the stellar interior when the temperature at the bottom of the convective layer reaches about 2×10^6 K (Bodenheimer 1965). There is evidence indicating that the lithium abundance is anticorrelated with age in late-type stars, which possess deep convective envelopes (Duncan, 1981).

The equivalent widths of the lithium line, W(Li)$_{hr}$, measured from the high-resolution spectra for our sample are reported in Table 2. The equivalent widths were obtained by integration performed by linear interpolation of the continuum on both sides of the absorption line using MIDAS. The mean estimated error is 0.015 Å in most cases. Only in very few cases of late-type spectra and low S/N, the uncertainty may be as high as 0.05 Å. Concerning the problem of line blending and photospheric continuum placement due to rotation, we note that this effect may become important for $v \sin i$ larger than 60 km/s. However, such fast rotators are not common in our sample (see Fig. 8) and they are mostly found among earlier spectral types, which will not be considered when deriving a lower limit for the number of "bona-fide" PMS stars (see Sect. 7.2).

It is useful to compare the new determinations with previous results (W(Li)$_{lr}$) obtained in Paper I from medium/low resolution spectra of the same stars, since the uncertainty on the latter determinations was rather high mainly due to the unresolved blend with the nearby iron lines (FeI $\lambda\lambda$ 6703, 6705 and 6710 Å), as well as to indetermination in positioning the stellar continuum.

Fig. 3a shows the equivalent widths derived from low-resolution spectra versus those obtained from high-resolution ones. It is clearly seen that, apart from a wide spread, there seems to be a general systematic tendency to overestimate the equivalent width from low resolution spectra, and the relative error can be indeed quite large, especially at low values of lithium line strength. In particular, the detection limit for lithium from low-resolution data is about 0.15 Å equivalent width, slightly depending on spectral type as well as on the resolution used. In particular, this problem has been pointed out quite recently by Br97, and represents one of the major arguments in support to their model, predicting that most of the stars detected in the RASS and previously classified as WTTS on the basis of low-resolution spectroscopy are not PMS stars, but somewhat older (about 10^8 yr) ZAMS stars.

The importance of the blend of the Li 6708 Å line with Fe I lines, as well as the indetermination on positioning of the continuum are expected to vary with spectral type. Thus, it is convenient, in order to highlight the spectral type dependence, to examine how the relative difference depends on effective temperature. In Fig. 3b, the ratio $(W(Li)_{lr} - W(Li)_{hr})/W(Li)_{hr}$ is plotted against the effective temperature of the star. What we can infer from this plot is that the major sources of error on the lithium equivalent width are different for different spectral types. In particular, for spectral types earlier than about G0, the lithium line, appears normally weaker, and thus the uncertainty on the equivalent width measured on low-resolution spectra is correspondingly larger. This, presumably, makes the effect of detection bias on low resolution spectra higher at these spectral types. In K type stars the iron lines strengthen, thus the blending effect with the lithium line becomes more important; in M types, the major source of uncertainty comes instead from the positioning of stellar continuum, and this may explain the larger scatter of measurements around zero.

It is however important to mention that recent studies on lithium in active late type stars and RS CVn candidates, selected on the basis of Ca II H and K emission, have shown enhanced lithium abundance with respect to field stars (Pallavicini et al. 1992). Whether this is due to stellar youthness or to the high level of activity it is not perfectly clear, even if there seems to exist some evidence for a lithium-activity correlation in K dwarfs probably as a result of the age dependence of these two quantities (Favata et al. 1996).

5. Radial velocity determinations

Radial velocity determinations have been performed through cross correlation analysis of the stellar spectra with those of radial velocity standard stars, treated in analogous way. Given the large spectral range covered, the cross correlation was performed after rebinning the spectra to a logarithmic wavelength scale, in order to eliminate the dependence of Doppler shift on the wavelength (Simkin, 1974). Moreover, only parts of the spectra free of emission lines and/or not affected by telluric absorption lines have been used. Therefore, the NaI D, and Hα lines as well as wavelengths longer than about 7000 Å have been excluded from the cross-correlation analysis. Typical cross-correlation functions for a single and a spectroscopic binary are shown in Fig. 4.

The heliocentric radial velocities for the sample are reported in Table 2.

6. $v \sin i$ determinations

Projected rotational velocities, $v \sin i$, for the sample in Chamaeleon have been determined using both the Fast Fourier Transform (FFT) method applied to suitable photospheric line profiles and the cross correlation technique.

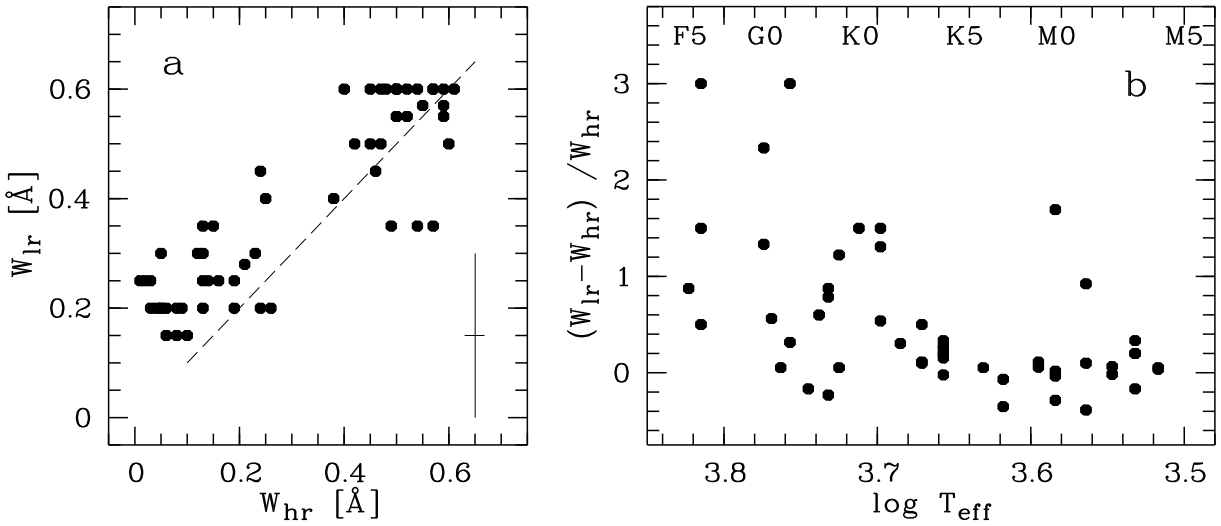

Fig. 3a and b. Comparison of lithium equivalent widths obtained from low and high-resolution spectroscopy. The left panel shows low-resolution versus high-resolution determinations, whilst in the right panel the relative error, e.g. the ratio $(W(Li)_{lr} - W(Li)_{hr})/W(Li)_{hr}$ is plotted against the effective temperature, in order to emphasize a possible dependence on spectral type.

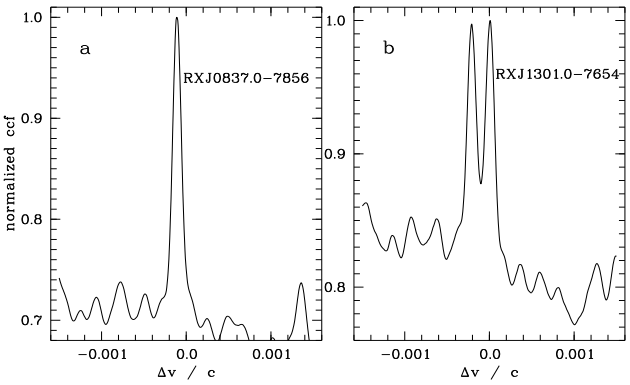

Fig. 4a and b. Examples of cross-correlation function for two of the target stars. In panel **a** RXJ 0837.0-7856; in panel **b** the double-lined spectroscopic binary RXJ 1301.0-7654. The abscissa gives the relative radial velocity shift, $\Delta v/c$, with respect to a reference radial velocity standard star.

6.1. Fourier transform method

We applied the Fourier transform analysis to extract the rotational broadening information from spectral line profiles and derive projected rotational velocities, using the analytical functional form for the rotation profile given by Gray (1976). The method relies on a few basic assumptions, namely, spherical symmetry, rigid body rotation and constancy of the intrinsic line profile across the stellar disk. As long as such assumptions are valid, the line profile of a rotating star can be expressed as the convolution of the line profile of a non-rotating star with an appropriate rotation profile. The limb-darkening effect is also taken into account by adopting the usual form of the limb-darkening law, $I_c = I_c^0[(1-\epsilon) + \epsilon\cos\theta]$, where ϵ is the limb-darkening coefficient (set to 0.6) and θ the angle between the direction normal to the stellar surface and the line of sight. The validity of all these assumptions has been exhaustively discussed by Bouvier et al. (1986).

We derived $v \sin i$ by applying the above method to the most suitable lines selected from the list provided by Franchini et al. (1988).

6.2. Cross-correlation method

In addition to the Fourier transform method, we used the correlation with a synthetic spectrum to determine $v \sin i$. The result of the correlation is a correlation peak which can be fitted with a gaussian curve. The parameters of the gaussian, center and full-width half-maximum (σ) are related to radial (V_{rad}) and rotational ($v \sin i$) velocities, respectively. The method of the correlation has been fully described by Queloz (1994), and Soderblom et al. (1989), and we will just describe the calibration procedures, and the error determinations, in Appendix A.

Correlation was applied with two different synthetic spectra corresponding to spectral types F0 and M0. For all the stars for which we could determine a velocity, mask M0 confirmed the existence, and the location, of the peak found with mask F0, and when no peak appeared with the F0 mask, no peak either appeared with M0, even for M type stars. So we performed $v \sin i$ determination only with the F0 mask, applied over the whole wavelength range. Results of the correlation method are reported in Table 2.

As a consequence of the gaussian fit, this method is more reliable for slow rotators, and, in a few cases, the correlation method failed to determine any velocity, because no clear correlation peak appeared from noise. Some stars have $v \sin i$ lower than our detection limit 5 of km s^{-1}. Some stars show emission lines (see Sect. 4), which leads to a noisy, or even undetectable,

Table 2: Equivalent widths of Hα and Li I λ 6708 Å, rotational and radial velocity determinations for the star sample in Chamaeleon. The last three columns, in the order, provide information on: the type of Hα line profile, according the classification scheme given in Sec. 4.1, the evolutionary status of the star, as derived by the lithium criterion introduced in Sec. 7.2, and, finally, a compact description of the most noticeable characteristics of each star.

Star RXJ	SpT	W(Hα) [Å]	W(Li I) (λ6708) $\pm$0.015 [Å]	vsin i $_{(FFT)}$ [km s^{-1}]	vsin i $_{(cross-corr)}$ [km s^{-1}]	RV $\pm$2 [km s^{-1}]	Evol. status	Hα profile	Notes
0837.0-7856	K4	-1.10	0.52	13±3	–	+18.0	PMS	3	
0842.4-8345	K6	-1.00	0.03	21±3	23±4	-8.0	?	3	
0842.9-7904	K4	-0.60	0.46	28±3	32±4	+4.3	PMS	4	
0844.5-7846	K7-M0	-1.10	0.52	<13	9±5	+15.0	PMS	4	
0848.0-7854	M2	-5.57	0.61	<13	13±3	+18.0	PMS	3	a
0849.2-7735	K1	+0.95	0.13	12±3	9±3	-3.4	?	1	
0850.1-7554	G6	+0.86	0.25	43±3	45±6	+15.5	PMS	2	
0853.1-8244	K0	+0.33	0.08	27±3	28±5	+7.7	?	2	
0902.9-7759	M3	-1.70	0.50	<18	17±6	+11.0	PMS	3	
0915.5-7609	K7	-1.15	0.54	20±3	–	+21.0	PMS	3	
0917.2-7744	G0	+1.30	0.15	60±3	54±10	+5.5	?	2	f: +12.7
0919.4-7738N	G3	+2.30	0.05	13±3	13±4	+3.2	?	1	
0919.4-7738S	G9	+0.05	–	37±3	35±5	+80.3	?	2	SB/a
0919.4-7738S	G ?	–	–	–	44±5	–	”	1	SB/b
0928.5-7815	F6	+4.50	0.10	140±5	–	+16.8	?	1	
0933.2-7433	M4	-8.70	0.00	13±2	12±4	+5.0	ZAMS	3	a,b,c
0935.0-7804	M2	-4.90	0.20	22±4	16±5	+14.0	PMS	3	a,b
0936.3-7820	G1	+2.60	0.16	20±3	19±4	+3.2	?	1	
0942.7-7726	M0	-2.16	0.49	<12	9±3	+16.4	PMS	3	a
0946.9-8011	M1	-4.30	0.05	80±5	78±7	+5.4	?	3	a, b, c
0951.9-7901	G7	-0.10	0.26	75±3	73±2	+12.2	PMS	2	
0952.7-7933	F6?	+3.30	–	22±10	12±9	+2.0	?	1	triple/a
0952.7-7933	F6	+3.30	–	34±10	19±6	+85.0	?	1	triple/b
0952.7-7933	F6?	+3.30	–	30±3	18±10	-98.0	?	1	triple/c
1001.1-7913	M0	-1.80	0.13	15±3	15±5	+12.2	PMS	3	a, b, c, e
1005.3-7749	M1	-2.80	0.57	11±3	–	+17.0	PMS	3	a,b
1007.7-8504	G0	-0.02	0.06	23±3	20±6	-67.1	?	4	f: +10.2
1009.6-8105	G8	+2.20	0.09	<13	6±4	+8.8	?	1	
1014.2-7636	M3	-8.14	0.00	20±3	23±4	+8.0	?	3	a, b, c
1014.4-8138	K7	-1.30	0.05	<12	11±5	+6.6	?	4	
1017.9-7431	G9	1.23	0.00	<10	<7	+104.0	ZAMS	1	f: +11.0
1035.8-7859	K7	–	0.00	12±3	8±3	+70.8	ZAMS	3	
1039.5-7538N	G3	+1.60	0.01	13±3	–	-3.4	?	1	
1039.5-7538S	G1	+1.40	0.03	38±3	40±5	-32.0	?	1	
1044.6-7849	M3	-2.40	0.00	14±2	<5	-8.4	ZAMS	3	a, b, c
1048.9-7655	K7	-1.53	0.00	16±3	15±3	-19.9	?	3	a, c
1108.8-7519a	K7	-1.70	0.33	20±3	23±5	+60.0	PMS	4	SB/a
1108.8-7519a	K7?	–	–	<12	14±6	-39.0	PMS	4	SB/b
1108.8-7519b	M3	-1.50	0.50	22±3	20±6	+11.0	PMS	4	a, c
1109.4-7627	K7	-0.74	0.59	14±3	15±3	+13.1	PMS	3	
B33	M3-4	-7.00	–	–	–	+13.0	?	3	a
F34	K3	-1.00	0.40	55±3	–	+14.0	PMS	4	e
1111.7-7620	K3	-7.30	0.50	23±3	–	+19.0	PMS	4	c, e; CHX18N
1112.7-7637	K4	0.00	0.47	11±3	–	+16.0	PMS	2	
1117.0-8028	M4	-11.77	0.57	21±3	–	+7.0	PMS	4	a, b, c
1120.3-7828	K6	-0.45	0.07	15±3	19±4	+134.0	?	4	SB/a
1120.3-7828	K6	-0.45	–	–	10±6	-26.3	?	4	SB/b
1123.2-7924	M1	-3.00	0.13	38±3	44±7	+10.0	PMS	4	a, c
1125.8-8456	F5	+4.00	0.08	30±3	41±5	+16.8	?	1	
1129.2-7546	K3	-0.23	0.45	21±1	20±3	+11.4	PMS	2	
1140.3-8321	K4	-0.16	0.21	15±3	13±4	+10.5	?	3	
1149.8-7850	M1	-32.0	0.50	18±5	13±5	+12.2	PMS	4	a, b, c, d
1150.4-7704	K4	-1.70	0.42	60±5	64±6	?	PMS	4	SB ?
1157.2-7921	G8	-2.70	0.38	39±3	–	+20.0	PMS	4	c, e; T Cha
1158.5-7754a	K4	-0.50	0.48	12±2	11±3	+13.1	PMS	3	
1158.5-7754b	M3	-2.90	0.60	<15	<5	+13.0	PMS	3	a, c
1158.5-7913	K6	-3.34	0.57	30±5	26±3	+13.1	PMS	3	a, c
1159.7-7601	K4	-0.39	0.50	<12	10±3	+13.1	PMS	3	
1201.7-7859	G5	1.20	0.24	21±3	21±3	+10.0	PMS	1	
1202.1-7853	K7-M0	-2.48	0.54	14±3	12±3	+5.0	PMS	3	a, b
1203.7-8129	K1	+0.63	0.12	11±3	–	-14.0	?	2	SB ?
1204.6-7731	M2	-4.20	0.47	<13	6±4	+10.4	PMS	3	a, b
1207.9-7555	K4	0.09	0.04	<11	9±3	-3.4	?	3	
1209.8-7344	K1	-0.10	0.11	16±3	–	+1.0	?	4	
1216.8-7753	M4	-4.00	0.55	<13	10±3	+14.0	PMS	3	a, b
1217.4-8035	G2	1.51	0.19	40±2	37±4	-13.0	?	1	f: +10.2
1219.7-7403	M0	-3.30	0.56	13±4	7±3	+13.1	PMS	3	a, b
1220.4-7407	M0	-2.24	0.53	45±3	41±3	+18.0	PMS	3	a
1220.6-7539	K2	-0.25	0.23	12±3	–	+6.0	?	3	
1223.5-7740	F6	3.20	0.06	30±3	26±4	+10.4	?	1	
1225.3-7857	G7	1.02	0.14	13±3	12±3	-6.7	?	1	
1233.5-7523	K1	1.41	0.13	<11	7±3	+14.0	?	1	
1239.4-7502	K3	0.07	0.40	20±3	19±3	+13.1	PMS	2	
1243.1-7458	M3	-3.90	0.45	25±3	27±6	+7.0	PMS	3	a, b, c
1301.0-7654	K4	-3.90	0.27	23±3	–	-21.0	PMS	3	SB/a
1301.0-7654	K4	-	0.28	20±3	–	+54.0	PMS	3	SB/b
1307.3-7602	K0	1.15	0.02	<10	<5	-62.8	?	1	f: +8
1325.7-7955	K1	+0.55	0.08	37±3	–	+30.0	?	1	SB/a
1325.7-7955	K ?	+0.55	–	?	–	-66.0	?	1	SB/b
1349.2-7549E	G3	+1.40	0.19	20±3	–	+1.0	?	1	
1415.0-7822	G7	0.00	0.24	42±3	–	+21.0	PMS	2	f: +11

notes to table:

a: He I (λ5876) in emission ; b: Na I D emission; c: [O I] emission; d: He I (λ6678) in emission;
e: Infrared excess emission; f: radial velocity of Na I D interstellar components in km/s

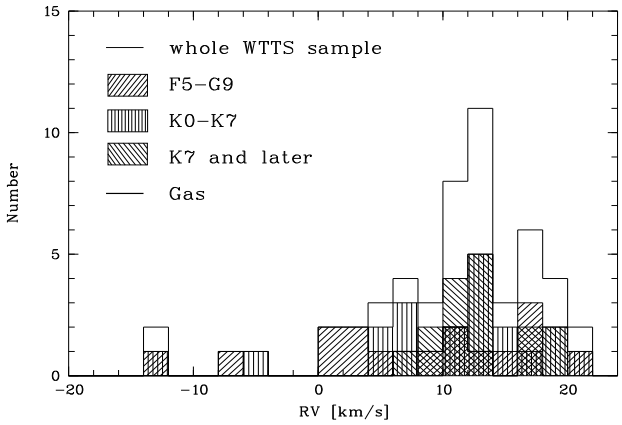

Fig. 5. Histograms of radial velocities for three different bins of spectral type. The thin solid line represents the whole sample.

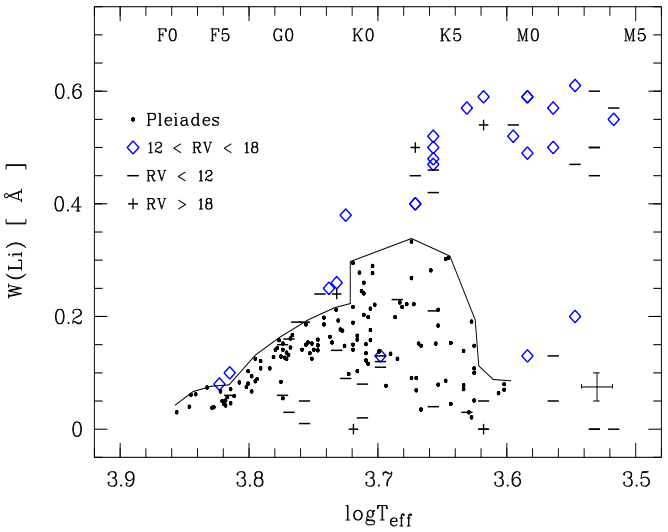

Fig. 6. Plot of the equivalent width of the Li λ 6708 Å, W(Li), versus the logarithm of the effective temperature, T_{eff}, for stars of the observed sample in three different bins of radial velocity: diamonds indicate stars with +12<RV /km s^{-1} <+18; minus and plus symbols represent stars with RV<+12 and RV>+18 km s^{-1}, respectively. The small black dots represent the Pleiades stars from Soderblom et al. (1993), and the solid line represents the upper envelope defined by their sample.

correlation peak (namely, RXJ 1014.2-7636, and RXJ 1117.0-8028).

The results obtained with FFT method and cross correlation technique match pretty well within the errors for intermediate rotational velocities. For low $v \sin i$ values (< 15 km s^{-1}), the rotational velocity was better determined by the cross correlation technique, whilst the FFT method was more suitably applied for measuring high rotation rates.

For the subsequent analysis of rotational velocity distributions, we will therefore use $v \sin i$ determinations obtained from the FFT method, for stars rotating faster then 15 km s^{-1} and from the cross-correlation for slower rotators.

7. Results

7.1. Radial velocities

Dubath, Reipurth & Mayor (1996, henceforth DRM96), have recently reported high-resolution data for a sample of 19 stars in the Cha I cloud. Here we use their results for comparison with our data.

Fig. 5 shows the distribution of radial velocities for the the stars in our sample. Also indicated in the figure are the distributions for the early-type (F5-G9) and late-type (later than K0) sub-samples.

The radial velocity distributions for the total sample and for the late-type sub-sample show a remarkable peak between +10 and +15 km s^{-1}, while apparently a flatter distribution of radial velocity is observed among the more scanty early-type sub-sample.

The observed radial velocity peak for the late type group is consistent with the radial velocity of the T Tauri stars in the Cha I dark cloud, as well as with the radial velocity of the gas in the Cha I cloud, as derived from CO observations (DRM96). The velocity dispersion appears however quite large, about 13 km s^{-1}, for the total distribution, and about 6 km s^{-1}, for the late-type sub-sample. Such a large velocity dispersion appears to be consistent with the fact that these stars are spread over a much larger volume than the cloud TTS population and might suggest that some of the early-type stars are unrelated to the star forming region.

In a few cases, the interstellar components of the Na I D lines are clearly distinguishable from the stellar absorption lines, because of a very different radial velocity shift of the star (e.g. RXJ 1017.9-7431, RXJ 1307.3-7602 and RXJ 1349.2-7549) and/or large rotational broadening of the photospheric lines (e.g. RXJ 0917.2-7744, RXJ 1007.7-8504 and RXJ 1217.4-8035). In the former case it seems very likely that we are dealing with background stars since they do not show any lithium absorption. In all cases, the radial velocity of this interstellar components gives us an estimate of the radial velocity of the gas in the correspondent line of sight and it is found to be in the range between 10 and 15 km s^{-1}.

Apart from the CO observations reported by DRM96 for the Cha I cloud, no other observations of the kinematics of gas in the Chamaeleon region are available from the literature. There is only one observation in the CO 1-0 transition toward the star RXJ 1157.2-7921 (T Cha) which gives an RV$_{LSR}$ = 4.5 km s^{-1}(Penprase, private communication), which corresponds to a heliocentric radial velocity of the gas of about 13 km s^{-1}.

For the subsequent analysis we will use as a reference the radial velocity distribution for the TTS of DRM96 sample in the Cha I cloud, assuming it is representative for the whole Chamaeleon region. Therefore, we regard radial velocities within the interval +12<RV/km s^{-1} <+18, which corresponds to the full radial velocity range observed for stars in the Cha I cloud (Fig. 3 in DRM96), as consistent with the radial velocities in the Chamaeleon SFR.

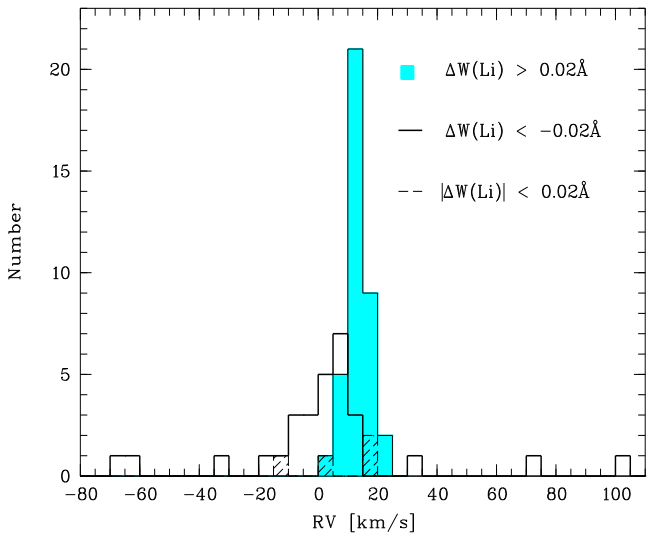

Fig. 7. Comparison of the radial velocity distributions for stars with lithium excess relative to the Pleiades and for weak-lithium stars.

7.2. Stars with strong lithium

In Fig. 6 we show a plot of the equivalent width of the Li λ 6708 Å, W(Li), versus the logarithm of effective temperature, T_{eff}, for stars of the observed sample, in the three different bins of radial velocity: +12 < RV/km s^{-1} < +18, RV < +12 and RV > +18 km s^{-1}. Following Magazzù et al. (1997), we also plot for comparison the Pleiades stars from Soderblom at al. (1993), as well as the upper envelope defined by their sample. It is quite striking that most of the stars with strong lithium absorption line do also have radial velocities which are apparently consistent with those found in the Cha I cloud by DRM96, while most of the stars with radial velocities out of that range fall well below the Pleiades upper limit, suggesting that they are probably unrelated to the SFR.

The distribution of radial velocities for the stars with lithium excess relative to the upper envelope for Pleiades stars (as defined below) is shown in Fig. 7 (shaded histogram). It is noticeable the well defined peak at 13 km s^{-1} which is consistent, within the errors, with the radial velocity measured for stars and gas in the Cha I cloud by DRM96. A gaussian fit to this distribution yields a velocity dispersion of 4 km/s for the stars with lithium excess. For comparison, the distribution for the stars falling below the Pleiades upper envelope is also drawn. The latter appears much broader suggesting that most of these stars may be completely unrelated to the Chamaeleon complex. One should note, however, that a few of them also have radial velocities apparently consistent with the star forming region and fall close to the Pleiades upper envelope (i.e., $\|\Delta W(Li)\| < 0.02$ Å), therefore, one cannot exclude the possibility that some of these stars are younger than Pleiades stars.

The above results indicate that our sample contains a mixture of at least two different populations of stars: one of very young, *bona-fide* PMS stars, the other of active dwarfs, probably unrelated to the Chamaeleon dark cloud complex. There are, however, also 10 stars with strong lithium, whose radial velocities are apparently inconsistent with the mean for Cha I. Most of them are later than K7 and, hence, have masses lower than 0.6 $M_{\odot}$ (derived by using the third set of PMS evolutionary tracks by D'Antona & Mazzitelli, 1994). None of these stars has been detected as a visual binary by Brandner et al. (1996) nor as a spectroscopic binary by us (see section 7.4). Four of these stars (namely, RXJ 1117.0-8028, RXJ 1158.5-7754b, RXJ 1202.1-7853, and RXJ 1243.1-7458) have radial velocity less than 10 km s^{-1} and may therefore represent good candidates for being "run-away T Tauri stars" (RATTS), according to the model proposed by Sterzik & Durisen (1995) to explain the presence of very young stars far from the main star forming clouds. We cannot exclude, however, that some of them might also be unrecognized spectroscopic binaries.

Using the above result that our sample contains a mixture of truly PMS and of active field dwarfs, (probably of Pleiades age and older) we consider these two groups separately for the analysis of the rotation properties. The two groups are defined by the value of the lithium excess, $\Delta W(Li) = W(Li) - W(Li)_{Pleiades}$, being greater than and, respectively, smaller than 0.02 Å (which is slighlty higher than the mean error on the high-resolution equivalent width measurements). In this way one can safely state that stars later than G5 with lithium excess higher than this value are truly PMS stars, considered that significant lithium depletion occurs in late type stars, having sufficiently a deep convective zone. For stars earlier than G5, no lithium depletion is observed in stars of different age (Pasquini et al. 1994, Favata et al. 1996), hence the lithium criterion is not valid anymore.

According to this "lithium criterion", 35 stars in our sample are confirmed to be *bona-fide* PMS stars out of 56 of spectral type later than G5. The remaining 21 stars show less lithium compared to the upper limit for Pleiades of the same spectral type and, therefore, most of them are probably not PMS stars.

This yields a percentage of 62 % PMS stars among the non-binaries late-type stars in our sample. Including also the spectroscopic binaries later than G5 having strong lithium (see Sect. 7.4), this percentage is 63 %. This result indicates that our original sample shows a contamination by older active field stars to an extent of about 37% for late-type stars (later than G5).

Considering the extreme case that all stars in our sample earlier than G6 are contaminating field stars, we obtain an upper limit for the contamination of 47%. Thus, more than 50% of the RASS WTTS candidates in Chamaeleon are confirmed to be PMS stars. If we relax our conservative limit on the value of $\Delta W(Li)$ to zero, the percentage of PMS stars raises to about 60%.

Interestingly, most of the stars which are confirmed PMS show Hα line profile of types 2, 3, and 4 described in Sect. 4.1, with a clear predominance of chromospheric and broad complex line profiles.

In the following, with the term WTTS we will refer only to those stars which have been confirmed to be PMS stars on the basis of the lithium criterion.

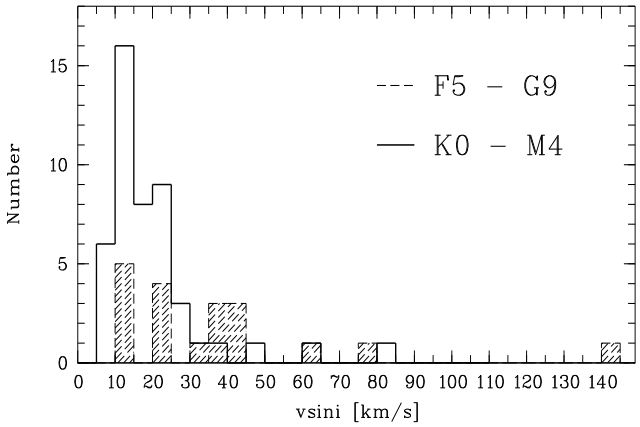

Fig. 8. Histograms of the projected rotational velocity for the two spectral type bins F5-G9 and K0-M. Spectroscopic binaries are excluded.

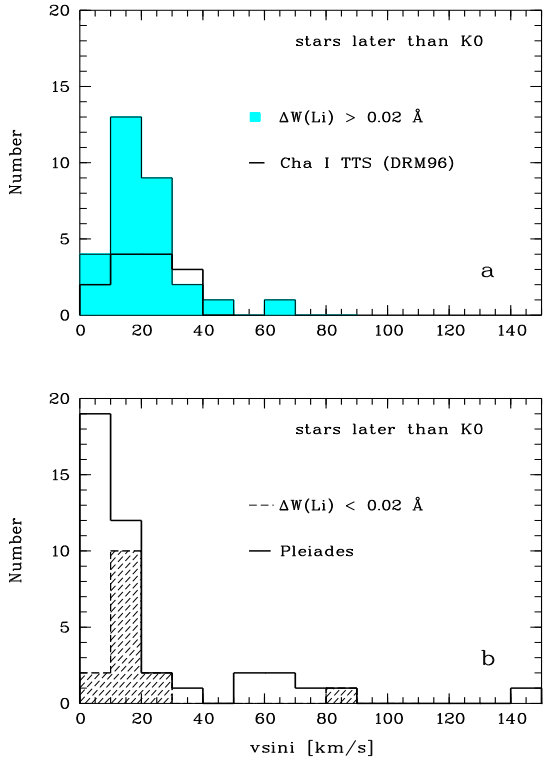

Fig. 9a and b. Distributions of rotational velocities for stars later than K0 for WTTS (top panel) and for non-WTTS stars (lower panel), compared with the $v \sin i$distribution for the TTS in the Cha I cloud (from Dubath, Reipurth & Mayor 1996) and with that for the Pleiades stars (from Soderblom et al. 1993), respectively. All known and suspected spectroscopic binaries have been excluded.

7.3. Rotation properties of the sample

Current models of the angular momentum evolution of young low-mass stars make the following predictions: i) close to the birthline, most of the stars are locked to a low rotational velocity as the result of the coupling between the star and its disk, ii) as the disk dissipates, the star is free to respond to its decreasing moment of inertia and consequently spins up as it contracts toward the ZAMS, iii) maximum rotational velocities are reached just before the stars reaches the ZAMS, onto which it is subsequently braked by its stellar wind.

The distribution of rotational velocities for the observed sample (excluding stars detected as spectroscopic binaries) is displayed in Fig. 8, for the two spectral type bins F5-G9 and K0-M.

To study the rotational properties of our sample, we have considered the two groups of stars defined according to the "lithium criterion", as described above. We compare the rotation properties of the strong-lithium group with those of "on cloud" TTS of the DRM96 sample in Chamaeleon, while the weak-lithium group is compared with the data for Pleiades stars from Soderblom et al. (1993). The distributions of rotational velocities for these different groups are shown in Fig. 9a and b (a and b). We restrict this comparison to stars of spectral class K0 or later in order to reduce the spread in $v \sin i$ introduced by the spectral type dependence of rotation (see Fig. 8), and we also exclude all recognized spectroscopic multiple systems. This cut in spectral type appears also consistent with the fact that the "lithium criterion", used here for discriminating PMS from other kinds of chromospherically active, but otherwise older stars, only applies unambiguously for late spectral types.

The comparison of the $v \sin i$ distribution of the Cha WTTS sample with that of the TTS sample in the Cha cloud observed by DRM96 shows that the two distributions are very similar to each other. This indicates that the two samples have quite close rotation properties, suggesting that they are probably in a similar evolutionary stage. The $v \sin i$ distribution of ROSAT WTTS (e.g. stars with $\Delta W(Li) > 0.02$ Å shown in the upper panel) is also strikingly similar to that of X-ray and optically selected pre-ROSAT WTTS located in dense dark clouds (Walter et al. 1988, Bouvier 1989). This distribution provides independent evidence that these stars are indeed in their earliest phase of their evolution. Most of the ROSAT WTTS have $v \sin i$ between 5 and 30 km/s, with a tail of faster rotators extending up to 60 km/s. In comparison, classical T Tauri stars have velocities less than 20 km/s (Bouvier et al. 1986, Hartmann & Stauffer 1989). The excess of fast rotators in WTTS compared to CTTS is explained in the models as resulting from the spin up of diskless young stars as they contract on their Hayashi tracks. At this early stage, stars have had little time to spin up, and no extreme velocities such as those observed on the ZAMS ($\simeq$ 200 km/s) are yet observed.

The $v \sin i$ distribution of the weak-lithium stars is similar to that of Pleiades late-type stars, with a number of slow rotators ($v \sin i <$ 15 km s^{-1}), and a sparsely populated tail of fast rotators. This suggests that most of the weak-lithium ROSAT

sources are evolving on the ZAMS. Most of these stars have $v \sin i$ in the range from a few km/s to 80 km/s and most likely are Pleiades-age field stars. The remaining few stars showing no lithium at all have $v \sin i$ less than 9 km/s and probably are much older contaminating field stars. The lack of slow rotators (e.g. $v \sin i <$ 10 km s^{-1}) among the ROSAT selected sample is most likely due to X-ray selection since the slowest rotators exhibit an X-ray emission which is too weak to be detected in the RASS.

We performed different two-sample tests using the program ASURV (vers. 1.2) as well as two-sided Kolmogorov-Smirnov tests in order to compare the four $v \sin i$ distributions shown in Fig. 9a and b, with the following results: the WTTS and Cha I TTS $v \sin i$ distributions are very similar to each other, while the WTTS and Pleiades $v \sin i$ distributions are very different; on the other hand, the weak-lithium stars $v \sin i$ distribution turns out to be somewhat in between the $v \sin i$ distributions of PMS and ZAMS stars. Thus, the weak-lithium sample contains stars with rotational properties which are intermediate between WTTS and ZAMS stars suggesting that they could be PTTS. However, this is not necessarily the case, since it might simply reflect the fact that all these stars have been selected on the basis of their X-ray emission and, hence, the sample is probably biased toward more active and faster rotating stars.

7.4. Spatial distribution

The analysis of the spatial distribution of radial velocities is useful to identify sub-groups of comoving stars in our sample. Fig 10 shows the spatial distribution of the stars in our sample. Three different symbols, namely, diamonds, minus and plusses symbols, are used to represent stars with radial velocities falling in each one of the following three radial velocity intervals: +12<RV /km s^{-1} <+18, RV<+12 and RV>+18 km s^{-1}, respectively as in Fig. 6. The stars with strong LiI (λ6708Å) absorption in their high-resolution spectra are marked with a hashed circle, whose size is proportional to the logarithm of the age (derived as in Paper II, but using the new spectral types).

Although the extinction is relatively low, we find that the stars with $A_V \geq 0.5$ mag are apparently more clustered, while the stars with less or almost no extinction, are more widely spread over the whole region. Interestingly, most of the stars with large excess of lithium (λ6708Å) relative to the Pleiades stars have extinction values $A_V \geq 0.5$ mag. Remarkably, the group of four stars located at about R.A. 08^h40^m and Dec $-78°50'$, have similar values of extinction as well as strong lithium relative to the Pleiades, and three of them also show similar radial velocity. These stars may be members of a small star forming region.

On the other hand, the stars with low extinction values and little or no lithium excess relative to the Pleiades appear more widely spread over the whole region and moreover, most of them have radial velocity inconsistent with the mean for Cha I. These stars can be candidates for older Pleiades-like objects. Assuming the 150 pc flat distance distribution as in Paper II, these stars turn out to be also older than the other more clustered stars with $A_V \geq 0.5$ mag and large excess of Lithium with respect to the Pleiades. Thus, the stars with RV consistent with the Cha I members, with low extinction values and little or no excess of Lithium relative to the Pleiades ($\|\Delta W(Li)\| < 0.02$ Å), are good candidates for being post-T Tauri stars.

The stars with $12 \leq$ RV/km s$^{-1} \leq 18$, as well as strong lithium and larger extinction apparently tend to follow more closely the large scale dust lanes of the 100μ IRAS emission, in the direction from the North-East ($\alpha \approx$ 13:00; $\delta \approx$ -75°) to the South-West ($\alpha \approx$ 8:00; $\delta \approx$ -80°). The intensity level of the contours traced in Fig.10, (without subtracting the background) corresponds to 16 mJy Sr^{-1}. Although this dust emission is very weak, it is an indication of the existence of residual matter in those regions. Some WTTS are located close to such weak IRAS emission regions, where no CTTS have been found so far. Also remarkable is the lack of stars with strong lithium in the southernmost region of about 3° in radius centered at $\alpha \approx 10^h : 15^m$ and $\delta \approx$ -83°, where no dust emission is observed and radial velocities are not consistent with the Cha I star forming region. In a new study based on RASS data in a strip perpendicular to the galactic plane which crosses the area in Chamaeleon studied in Paper I, there is also evidence for the presence of young low-mass PMS stars (Alcalá et al. in preparation).

These facts strengthen the evidence for the existence of groups of low-mass PMS stars far from the three main centers of the star forming region.

7.5. New spectroscopic binaries

Five stars out of 74 in the observed sample were found to be spectroscopic binaries and one resulted to be a spectroscopic triple. Namely, RXJ 0919.4-7738S, RXJ 1108.8-7519a, RXJ 1120.3-7828, RXJ 1301.0-7654, RXJ 1325.7-7955, are double-lined spectroscopic binaries, and RXJ0952.7-7933 is a three-component spectroscopic system.

Application of the lithium criterion to the spectroscopic binaries (triple) is not straightforward since one should take into account the contribution of the different components to the total continuum according to their spectral type. However, we more simply used the intensity of the Ca I λ 6718 Å as a reference to compare the lithium line strength for the two components. For the stars RXJ 1108.8-7519a and RXJ 1301.0-7654, the strength of the lithium line, for both components, is stronger than the corresponding nearby Ca I λ 6718 Å by a factor of about two, thus confirming their PMS nature. The stars RXJ 0919.4-7738S and RXJ 1325.7-7955 show relatively large rotational broadening of the lines, which make difficult to clearly distinguish the single components and derive accurate line equivalent widths. However, when comparing visually the Li λ 6708 and Ca I λ 6718 Å lines in these stars, they appear to have roughly the same strength. Thus, one cannot exclude the PMS nature for these two binaries. In the case of RXJ 1120.3-7828 the lithium line is definitely weaker than the Ca I line. Thus, since the star shows two well separated emission peaks at Hα, it is more likely an active binary rather than a PMS star. Finally, although the strengths of

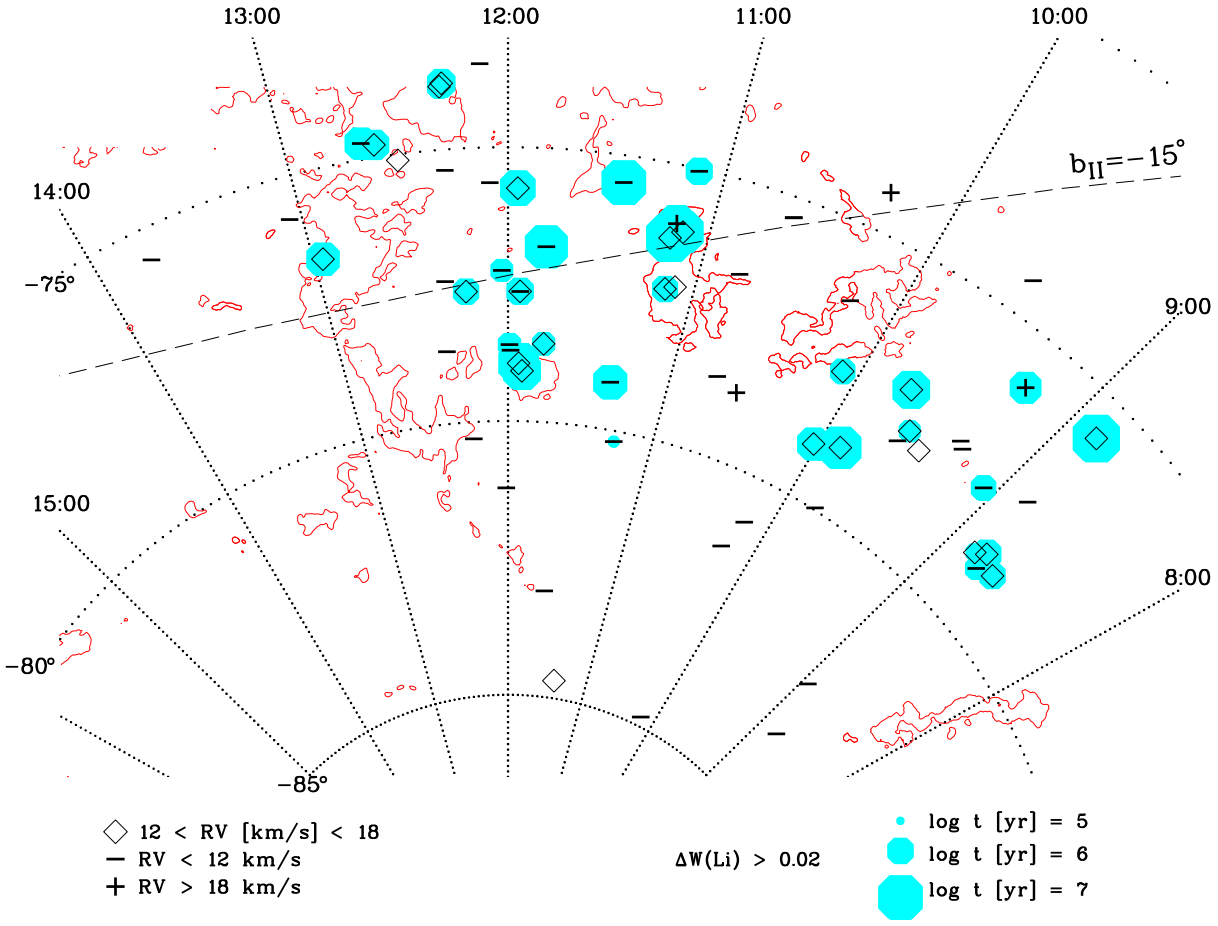

Fig. 10. Spatial distribution of the observed sample in three different radial velocity bins: diamonds indicate stars with +12<RV[km s^{-1}]<+18; minus and plus symbols represent stars with RV<+12 and RV>+18 km s^{-1}, respectively. Additionally, stars presenting a lithium excess, $\Delta W(Li) > 0.02$, (defined with respect to the upper limit for Pleiades stars) are marked with a shaded circle whose size is proportional to the logarithm of age. The dashed line traces the galactic parallel $b_{II} = -15°$.

the lithium components in the triple system RXJ 0952.7-7933 are stronger than the corresponding calcium components, the spectral type is too early (≈ F6) to establish the PMS nature on the basis of the lithium line.

One of the spectroscopic binaries, RXJ1301.0-7654, is also reported by Brandner et al (1996) to be a visual binary, with a separation of 1.43 arcsec. Thus, this star probably forms a hierarchical triple system. Only for this star we could collect repeated radial velocity measurements, which cover about half of the radial velocity curve, and we can then roughly estimate that the orbital period falls between 12 and 14 days. The two components of this spectroscopic binary have the same spectral type, and a mass ratio of about 1. This star is located on the Cha II dark cloud and the radial velocity of the barycenter of the system is about 11 km s^{-1}.

It is also likely that more spectroscopic binaries hide in our Chamaeleon sample, since for most of the objects we could obtain only one spectrum. Therefore, eventual single-lined spectroscopic binaries might have easily escaped to detection. Also, some apparently very fast rotators might actually be unresolved multiple spectroscopic systems. A few more stars are suspected to be spectroscopic binaries because of asymmetries present in the corresponding cross-correlation function, namely: RXJ 0849.2-7735, RXJ 0915.5-7609, RXJ 1158.5-7913, RXJ 1217.4-8035, RXJ 1220.4-7407. Thus, we estimate the actual close-binary fraction in the WTTS sample to be around 10%, or possibly higher.

8. Discussion

We have analysed the high-resolution spectroscopy of 74 stars classified as WTTS widely spread in the direction of the Chamaeleon complex and found on the basis of the RASS.

The main basis for the selection of this sample, apart from the high level of coronal activity, was the presence of the Li I λ 6708 Å absorption line on low-resolution spectra. As discussed in Sect. 4.1, low spectral resolution may lead to a systematic overestimate of the strength of this line, because of blending

with nearby Fe I lines and indetermination on the stellar continuum definition. This immediately leads to the question whether some of the stars in the sample classified as WTTS are in reality older, maybe Pleiades-like stars, as predicted by the Br97's model. Br97 also note a bimodal Lithium distribution and infer that the high Li stars are indeed WTTS, however, they conclude that most of the stars discovered with the RASS in SFR's are old enough (10^8 yr) to have dispersed far from their birth places in molecular clouds, producing a relatively homogeneous distribution of X-ray sources near the galactic plane.

The results we report here indicate that the stars in the sample of RASS WTTS defined by previous investigations in Chamaeleon (Paper I and II) to be a mixture of at least two distinct populations of stars: one of *bona-fide* PMS low-mass stars, the other, more heterogenous, probably composed by older chromospherically active, field dwarfs (most of which probably Pleiades-like). However, we do not find evidence that most of the lithium stars detected by the RASS in the Chamaeleon region are ZAMS stars, in contrast to the predictions of the model by Br97. Analogous findings are coming from investigations in other star forming regions. In particular, high resolution spectroscopy of ROSAT WTTS candidates in the Lupus SFR yields indication of quite low contamination from active field stars (Wichmann et al., in preparation). This suggests that the results may differ from one region to the other, probably due to differences in the small scale structure of different SFR. Being conservative, we find that more than 50% of the investigated sample in Chamaeleon are instead confirmed to be truly young PMS stars and they do not appear homogeneusly distributed over the investigated area, but seem to trace preferentially the direction of the 100μ IRAS dust emission lanes (see Fig. 10) from North-East ($\alpha \approx 13^h$; $\delta \approx -75°$) to South-West ($\alpha \approx 8^h$; $\delta \approx -80°$), which would approximately coincide with the direction of the hypothetic HVC proposed by Lépine & Duvert (1994) for the formation of the Chamaeleon complex.

The heterogeneous "contaminating" sample of active field stars appears instead more uniformly distributed and represents about 40% of the sample investigated with high-resolution spectroscopy. This means some 30 stars, out of the 77 in the original WTTS sample reported in Paper I, over an area of about 170 square-degrees. This corresponds to a number density of "contaminating" stars of ≈ 0.2 stars/square-degree. If we restrict to the spectral type interval G0 to late K, we find that the contaminating stars should then be 24 out of 51 stars. This yields a number density of about 0.15 G0-late-K stars per square degree, which is less than the value of 0.2-0.3 stars per square degree predicted by the Br97 model. Assuming that these stars (all having $\Delta W(Li) < 0.02$ Å) are active ZAMS stars, the resulting distance distribution covers a range from 30 to 200 pc with a mean distance of about 100 pc and a standard deviation of 40 pc. Hence, these stars probably correspond to the population predicted by Br97, although one cannot exclude that some of them might be younger than Pleiades (also to be expected from a constant star formation rate over 100 Myr, as assumed in the Br97 model). Determinations of trigonometric parallaxes for these stars, for example from the Tycho satellite data base, will allow to settle this question.

The apparent contradiction between the observations and the predictions of the model by Br97 should be probably sought for in the hypothesis on which this model is based. In particular, the basic assumptions of star formation spatially uniform and steady in time appear reasonably applicable only on average, over a large, galactic scale; however, they become less realistic when the comparison is restricted to a very special direction such as that of an active star formation region (cf. Palla & Galli 1997). It is important to point out that, although very large areas have been investigated so far on the basis of the RASS all around SFR's, they are still small to be considered on a galactic scale as it is done in Br97. And, since these RASS investigations are still spatially biased towards SFR's, the probability to find X-ray emitting PMS stars is higher than when considering an average over large galactic scale.

Another reason for the inconsistency of the observed number of *bona-fide* PMS stars with that predicted by Br97 may arise from the fact that the X-ray luminosity-age relation and the X-ray luminosity function they assume tend probably to underestimate the number of $\approx 10^7$ yr old stars. This is possibly due to the fact that Br97 restrict their sample of X-ray data to TTS with masses below 1.5 solar masses and A_V smaller than 1 mag. This obviously introduces a bias toward low X-ray luminosity objects. Another possible explanation is that Br97 do not include in their model the rotation-related X-ray detection bias for Pleiades-like stars. Therefore, their model predicts a lot of Pleiades-like contaminating stars. However, most of these stars will have $v \sin i < 10$ km s^{-1}, and will remain undetected in the RASS, because most of them are slow rotators (based on the Pleiades $v \sin i$ distribution) and, hence, weak X-ray emitters. Therefore, there must be many foreground Pleiades like stars in the surveyed area, as predicted by Br97 model, but only a minor fraction of those are actually detected in the RASS.

Since the "contaminating" sample is more heterogeneous and we are interested on the Chamaeleon PMS stars, for the rest of the discussion we concentrate on the more well defined *bona-fide* PMS stars, observed with high resolution spectroscopy, to trace the star formation history in the Chamaeleon region. This sample of *bona-fide* PMS stars, excluding the spectroscopic binaries, comprises 37 stars later than G5. Assuming for these stars an average distance of 150pc and using the D'Antona & Mazzitelli's (1994) PMS evolutionary tracks with Alexander opacities, their masses range from 0.25 to 1.7 $M_\odot$, and their ages from a few 10^5 to 10^7 yr, with 70% being younger than 5×10^6 yr. The age distribution of these stars shows a significant peak at 10^6 yr, which is consistent with the mean age determinations for the Cha I and Cha II members (Lawson et al 1996; Paper II). Furthermore, from the point of view of the rotational properties, the sample of *bona-fide* PMS stars also appears to show a behavior which resembles very closely that of the pre-ROSAT WTTS found in the in Cha I cloud and in other molecular clouds, providing an independent evidence that these stars are in a similar evolutionary stage.

When looking at the IRAS 100 μm map, the Chamaeleon region reveals several filamentary structures which extend over an area even larger than the one investigated on the basis of RASS data. Thus, one should expect that the star formation process took place in different parts of the region. However, no particular trend is observed for the younger PMS stars in our sample to be located more close to the main Chamaeleon clouds or to other regions of IRAS dust emission (c.f. Fig. 10). The existence of some very young stars far from the canonical centers of star formation is then confirmed. Thus, it is indeed necessary to invoke also other mechanisms than the dispersal of PMS stars by slow drifting from dense cloud cores, in order to explain the origin of these stars.

Sterzik & Durisen (1995) have proposed that some low-mass stars might be run-away T Tauri stars, ejected from the cloud cores by three-body encounters. However, it is difficult to explain the large fraction of PMS stars observed. This mechanism might explain the presence of a few, very young, single stars found relatively far from the main Chamaeleon star forming clouds, and showing radial velocity inconsistent with the mean for the SFR. Proper motion studies would also be necessary in order to address this issue.

According to a recent model proposed by Feigelson (1996), star formation may take place *in-situ* in short-lived cloudlets in turbulent giant molecular clouds, having velocity dispersions of ± 5 up to ± 10 km s^{-1}. This hypothesis finds some support in the kinematics of the *bona-fide* PMS stars in Chamaeleon, since it is apparently consistent with the velocity dispersion we observe for these stars. A striking example, as also noticed by Feigelson (1996), is represented by the group of four stars located at R.A. 08^h40^m and Dec $-78°50'$, which are definitely young, but far from any dense star forming cloud. CTTS would also be expected to form in such cloudlets, in which case one should reveal some CTTS far from the molecular clouds as well. There are indeed a few known cases of CTTS isolated from any molecular cloud, the most famous of which being TW Hya (Rucinski & Krautter 1983). However, we do not find any clear evidence for the presence of CTTS among the widely spread PMS stars in Chamaeleon, although investigations based on the IRAS point source data base have revealed a number of off-cloud T Tauri star candidates (Gregorio-Hetem et al. 1992; Torres et al. 1995). One of these objects coincides with RXJ 1149.8-7850, which is one of the most active stars in our sample, with strongly variable Hα emission. On the other hand, it has long been suspected that Bok globules are sites of isolated low-mass star formation (Bok & Reilly 1947). Recent studies (Launhardt 1996), have shown that 16 of 60 isolated globules can be associated with embedded IR and IRAS point sources in which very young stars (or protostars) and somewhat older young stars (TTS) are found. Whether Bok globules are related to the cloudlets of the Feigelson's model is not clear.

If the star formation rate were constant over the entire lifetime of a molecular cloud (e.g. of the order of 10 Myr), then one should expect a substantial fraction of PTTS among the RASS PMS stars (Feigelson 1996). However, although one cannot exclude that there might be a few stars younger than Pleiades among the "contaminating" sample with radial velocity consistent with Chamaeleon (see Fig.7), we do no find a clear evidence for the presence of PTTS stars in our sample. First of all, most of the *bona-fide* PMS stars in our sample turn out to be younger than 5×10^6, and second, we also notice a clear lack of stars in the so-called "PTTS gap" (Martìn 1997) in the W(Li)-log T_{eff} diagram for log T_{eff} lower than about 3.65 (see Fig.6). A possible explanation might be that the time scale for initial lithium depletion in late-type stars is relatively shorter, compared to the duration of the PMS phase, in lower mass stars where the convection zone extends more deeply into the stellar interior.

From considerations on the relevant time-scales for formation and evolution of molecular clouds and comparison with the typical time-scales for protostellar accretion and cloud dispersal, Palla & Galli (1997) argue that star formation is a slow process and that the time required for the onset of star formation may represent a substantial fraction of the entire lifetime of a cloud. On this basis, they conclude that the star formation rate of molecular clouds is not constant nor continuous in time but steeply rising with time during the typical lifetime of a molecular cloud (of the order of 10 Myr), and that the age spread observed among stars in a given molecular cloud is simply a consequence of spatial fluctuations in the physical conditions in the cloud ambient medium. Thus, the probability to find a large fraction of PTTS in a given star forming region is very low.

We point out that from our previous investigations on the Chamaeleon region (Paper I and II), we could not identify unambiguously PTTS among the RASS sample but, rather, we called the attention on the fact that some very young stars were found far from the main cloud cores (see the discussion about the age distribution in Paper II).

The presence of widely distributed young stars in SFR's can probably be explained in terms of triggered star formation. For the Chamaeleon SFR, there is no evidence of supernova events or for the presence of OB associations. Lépine & Duvert (1994) have proposed a hydrodynamical model in which a high-velocity cloud (HVC) with a velocity of about 100 km/s colliding with the galactic plane at an inclination angle of about 65° could be responsible for the large scale filamentary structure of the Chamaeleon cloud complex. It is suspected that the Chamaeleon T Tauri stars are moving towards lower galactic longitudes (in direction l = 300° to l = 280°) with a few km/s, almost parallel to the galactic plane, and thus, one would not expect the presence of T Tauri stars on the eastern side of the complex (Lépine 1996, private communication). In this scenario, one should expect the whole Chamaeleon complex (gas, dust and stars) to share a similar radial velocity component. Some observational facts seem to support this hypothesis: *i)* the widely spread PMS stars in Chamaeleon move with similar RV as the Cha I cloud and its PMS stars; *ii)* the star T Cha, located at the edge of the cloud FS 195 (Hoffmeister 1958) also has a RV consistent with the Cha I SFR. The RV of the FS 195 cloud, as measured by the interstellar NaI D components in the high-resolution spectra of the star T Cha, is RV=13.6$\pm$2.5 km/s (Franchini et al. 1992), also consistent with a CO observation

toward T Cha. Thus, this cloud also has a RV consistent with the Cha I cloud; *iii)* the RV of the barycenter of the spectroscopic binary RXJ1301.0-7654, located in the Cha II cloud, also is consistent with the RV of the Cha I cloud and thus, it is likely that also the Cha II cloud moves with a similar RV as the Cha I cloud; *iv)* in the spectra of the six stars in which the interstellar components of the Na I D lines can be distinguished from the stellar absorption lines (see Sect. 7.1), the RV of the gas is found to be in the range between 10 and 15 km s^{-1}, again consistent with the mean for Cha I.

The fact that the entire complex of clouds, filaments, on and off-cloud PMS stars in Chamaeleon seem to share a common motion suggests that they have probably a common origin which might be related to the impact of a HVC. This HVC impact might be responsible for the formation of the three main Chamaeleon clouds, of the filamentary structures observed in the complex, as well as for induced star formation in short-lived cloudlets which have dissipated, giving rise to the observed, widely dispersed PMS population.

9. Summary and conclusions

We presented high resolution spectroscopy for WTTS candidates in the Chamaeleon SFR. Our sample sums up to 74 stars, 60 of which with spectral type later than G5 and the remaining from F5 to G5. We obtain radial and rotational velocities and determine Li λ 6708 Å equivalent widths for all these stars. Projected rotational velocities, $v \sin i$, for the sample have been determined using both the Fast Fourier Transform (FFT) method applied to suitable photospheric line profiles and the cross-correlation technique.

More than 50% of the stars (and more than 60% in the late-type group) result to be *bona-fide* PMS stars showing significant lithium excess with respect to their young main sequence counterpart. Five new spectroscopic binaries and one spectroscopic triple are found and at least two of the late-type systems are confirmed to be PMS stars.

Our observations reveal that the studied sample is actually a mixture of two different populations of stars: one of "bona-fide" PMS low-mass stars, the other, more heterogeneous, probably composed by active, field stars. The observations however confirm that the majority of the late-type stars selected on the basis of the ROSAT survey are really young (ages less than 5×10^6 yr) , low-mass PMS stars and that these stars appear distributed over a broad strip tracing preferentially the direction of the 100μ IRAS dust lanes. The result from the previous RASS investigations in the Chamaeleon SFR that very young stars (age $\approx 10^6$ yr) are found far-off the Cha I, Cha II and Cha III molecular clouds, is definitely confirmed. On the other hand, we do not find any clear indication for the presence of PTTS among the RASS WTTS. The heterogeneous sample of "contaminating" active field stars appears instead more uniformly distributed. A sub-sample of these stars probably corresponds to the Pleiades-like stars predicted by the Br97 model but, as we conclude from our study, they do not represent the majority of the sample in this particular area.

Even if the RASS is spatially complete, and large areas toward SFR's have been already surveyed by optical follow-up observations, they are still small to be compared with models based on the assumptions that star formation is spatially uniform and steady in time. Thus, instead of a dominant population of active ZAMS stars, one should expect the PMS RASS samples to be just contaminated by such stars. Of course, such contamination should be expected to become more important at larger distance from the star formation complex.

The fact that the entire complex of clouds, filaments, on and off-cloud PMS stars in Chamaeleon seem to share a common motion suggests that they have a common origin, probably related to the impact of a HVC.

Acknowledgements. We wish to thank Dr. Andreas Juttner for providing us with MIDAS procedures for reduction of echelle spectra. We also thank D. Queloz and J.C Mermilliod for providing us cross-correlation software, synthetic masks and standard's $v \sin i$. Most of this work has been carried out while EC has been visiting the MPE in Garching and stimulating discussions with Drs. Michael Sterzik, Ralph Neuhäuser, and Jürgen Schmitt are widely acknowledged and we also thank Rainer Wichmann for comments on an earlier version of the paper. We thank the referee, Dr. Lee Hartmann, for his comments and constructive criticism. The use of reduction facilities at ESO Garching is also acknowledged. One of the authors (JMA) acknowledges a fellowship from MPE. The ROSAT project has been supported by the Bundesministerium für Bildung, Wissenschaft, Forschung und Technologie and the Max-Planck-Gesellschaft.

Appendix A: calibration procedure for the cross-correlation method

The star HD80170 ($v \sin i$=0.5 km s^{-1}) is used as a calibrating star. Its spectrum is convolved with rotational profiles (see Gray, 1976) of different rotational velocities, and the correlation procedure is applied to the resultant spectra. The result of the correlation (σ) is then plotted against the velocity and from the relation σ- $v \sin i$, we deduce the calibration relation. We used two spectra of the same star, for which we calibrated the relation from 0.5 to 40 km s^{-1}. The result is:

$$v \sin i = 1.796\sqrt{\sigma^2 - 7.114^2} \quad \text{(A1)}$$

The correlation method introduces different sources of errors: the gaussian fit which means an error on σ, and calibrations on $v \sin i$. The uncertainty introduced by the calibration is determined with the use of other rotational standards in the following way. We use Eq. A1 to derive $v \sin i$ for standard stars, and the statistics on the difference between this determination and the $v \sin i$ from literature lead to a dispersion of 3 km s^{-1}.

As prescribed by Queloz (1994), the uncertainty on the fitted parameters of the gaussian is a function of the depth of the gaussian (called D), and of the S/N ratio of the spectrum. For each spectrum of our sample, we generated 1000 artificially noisy spectra. The statistics on the fitted parameter σ of these

spectra gives the error on this parameter. A linear fit gives

$$\delta(\sigma) = 0.45 \frac{1}{D\frac{S}{N}} \ .$$

From Eq. A1, the uncertainty on $v \sin i$ is:

$$\delta(v \sin i) = 3 + 1.796 \frac{\sigma \delta(\sigma)}{v \sin i}$$

We also have to take into account that if $v \sin i$ becomes too large, the shape of the correlation peak is not a gaussian anymore, and this typically begins with $v \sin i = 40$ km s^{-1}. For greater $v \sin i$, there is a significant deviation between the velocity prescribed by the rotational profile and the velocity derived from the fit. Differences between the "true" $v \sin i$ and the $v \sin i$ calculated from Eq. A1 for the standard HD80170, for velocities greater than 40 km s^{-1}, lead to a supplementary uncertainty of $\delta(v \sin i)_{fit} = 0.13 v \sin i - 5.2$.

References

Alcalá J.M. 1994 PhD thesis, Universität Heidelberg

Alcalá J.M., Krautter J., Schmitt, J. H. M. M., Covino E., Wichmann R., Mundt R. 1995 A&AS, 114, 109 [Paper I]

Alcalá J.M., Krautter J., Covino E., Neuhäuser, R., Schmitt, J.H.M.M., Wichmann R. 1997 A&A, 319, 184 [Paper II]

Alcalá J.M., Terranegra, L., Wichmann R., et al. 1996 A&AS, 119, 7

Bodenheimer P. 1965 ApJ, 142, 459

Bok B., Reilly E. 1947 ApJ, 105, 255

Bouvier J. 1989 in: Rotation and Mixing in Stellar Interiors, eds. H. Araki et. al., Lect. Notes in Phys. 366, 47

Bouvier J. 1994 in Cool Stars, Stellar Systems, and the Sun, Eight Cambridge Workshop ASP Conference Series, Vol. 64, p 151

Bouvier J., Bertout C., Benz W., and Mayor M. 1986 A& A, 165, 110

Bouvier J., Forestini M. 1994 in Circumstellar Dust Disks and Planet Formation, eds. R. Ferlet, A. Vidal-Madjar, p. 347

Bouvier J., Cabrit S., Fernández M. et al 1993 A& A, 272, 176

Bouvier J., Covino E., Kovo O. et al. 1995 A& A, 299, 89

Bouvier J., Wichmann R., Grankin K. et al. 1997 A& A, 318, 495

Briceño C., Hartmann L.W., Stauffer J.R. et al. 1997 AJ, 113, 740 [Br97]

Brandner W., Alcalá J.M., Kunkel M., Moneti A., Zinnecker H. 1996 A& A, 307, 121

Choi P.I., & Herbst W. 1996 AJ, 111, 283

D'Antona F., Mazzitelli I. 1984 A& A, 138, 431

D'Antona F., Mazzitelli I. 1994 ApJS, 90, 467

Dubath P., Reipurth B., Mayor M. 1996 A& A, 308, 107 [DRM96]

Duncan D. 1981 ApJ, 248, 651

Favata F., Micela G., Sciortino S. 1996 A& A, 311, 951

Feigelson E.D. 1987 in Protostars and molecular clouds, eds. Th. Montmerle and C. Bertout (CEN Saclay, Gig-sur-Yvette), p.123

Feigelson E.D. 1996 ApJ, 468, 306

Feigelson E.D., Casanova S.E., Montmerle T., Guibert J. 1993 ApJ, 416, 623

Franchini M., Covino E., Stalio R., Terranegra L., Chavarria C. 1992 A& A, 256, 525

Franchini M., Magazzù A., Stalio R. 1988 A& A, 189, 132

Gray D.F. 1976, "The observation and analysis of stellar photospheres", Wiley & Sons, Inc., 394

Gregorio-Hetem J., Lépine J.R.D., Quast G.R., Torres C.A.O., de la Reza R. 1992 AJ, 103, 549

Hartmann L.W., Stauffer J. 1989 AJ, 97, 873

Jacoby G.H., Hunter D.A, Christian C.A. 1984 ApJS, 56, 257

Keppens R., MacGregor K.B., and Charbounneau P. 1995 A& A, 294, 469

Krautter J. 1996 in Cool Stars, Stellar Systems, and the Sun, 9^{th} Cambridge Workshop ASP Conference Series, R. Pallavicini & A. Dupree eds., Vol. 109, p. 395

Krautter J. et al. 1994 Rev. Mex. de Astron. y Astrofis. 29, 41

Krautter J., Wichmann R., Schmitt J.H.M.M., et al. 1997 A&AS, in press

Kunkel M. 1996 PhD Thesis, Universität Würzburg

Launhardt R. 1996 PhD Thesis, Universität Jena

Lawson A.W., Feigelson E.D., Huenemoerder D.P. 1996 MNRAS, 280, 1071

Lépine J., Duvert G. 1994 A& A, 286, 60

Magazzù A., Martín E.L., Sterzik M.F., Neuhäuser R., Covino E., Alcalá J.M. 1997 A&AS, in press

Martín E.L. 1997 A&A, in press

Pallavicini R., Randich S., Giampapa M. 1992 A&A 253, 185

Palla F, Galli D. 1997 ApJ Lett., 476, L35

Pasquini L., D'Odorico S. 1989 ESO Operating Manual No. 2

Pasquini L., Liu Q., Pallavicini R. 1994 A& A, 287, 191

Queloz D. 1994, in IAU symposium 167, Ed. A.G Davis Philip, p. 221

Rucinski S.M., Krautter J. 1983, A& A, 121, 217

Simkin S.M. 1974 A& A, 31, 129

Soderblom D.R., Jones B.F., Balachandran S. et al. 1993 AJ, 106, 1059

Soderblom D.R., Pendleton J., Pallavicini R. 1989, AJ 97, 539; erratum: vol. 98, 737

Sterzik M.F., Durisen R. 1995 A& A, 304, L9

Strom K.M., Wilkin F., Strom S.E., Seaman R.L. 1989 AJ, 98, 1444

Torres C.A.O., Quast G.R., de la Reza R., Gregorio-Hetem J., Lépine J.R.D. 1995 AJ, 109, 2146

Verschueren W., Hensberge H. 1990 A& A, 216, 216

Walter F. M.: 1992, AJ, 104, 758

Walter F.M., Brown A., Mathieu R.D., Myers P.C., Vrba F.J 1988, ApJ, 96, 297

Whittet D.C.B., Assendorp R., Prusti T., Roth M., Wesselius P.R. 1991 MNRAS, 251, 524

Wichmann R., Krautter J., Schmitt J.H.M.M., et al. 1996 A& A, 312, 439

Wichmann R., Krautter J., Covino E., Alcalá J.M., Neuhäuser R., Schmitt J.H.M.M. 1997 A& A, 320, 185

This article was processed by the author using Springer-Verlag LaTeX A&A style file *L-AA* version 3.